Aeroacoustics Conferences
June 14-17, 2022, Southampton, UK
28th AIAA/CEAS Aeroacoustics 2022 Conference
10.2514/6.2022-3097

Preliminary Results of Modal Analysis for a Ducted Axial Fan from External Pressure Measurements

Courtney Ford*
Ecole Centrale de Lyon, Ecully, France, 69134

Antonio Pereira†
Ecole Centrale de Lyon, Ecully, France, 69134

Christophe Bailly‡
Ecole Centrale de Lyon, Ecully, France, 69134

Identifying the modal content of a ducted fan of unique geometry based on measurements of the radiated pressure, the so-called inverse problem, requires the determination of transfer functions between modes running through a conduit and the chosen microphone array. This study describes the preliminary steps taken in determining the transfer functions between the LP3 engine housed at the Ecole Centrale de Lyon and the geodesic dome of microphones external to this duct. The transfer functions are then used to reconstruct the modes propagating from the engine inlet for the first three blade passing frequencies. These results are then compared to mode reconstruction accomplished from an in-duct microphone array, and it is determined that both methods identify the same dominant modes.

I. Nomenclature

$\mathbf{c}$	=	solution coefficients of the mode amplitudes in vector form
$\hat{c}_l$	=	solution coefficient of the l-th mode
$\hat{c}_i$	=	i-th element of vector $\mathbf{c}$
f	=	frequency
m	=	azimuthal mode order
n	=	radial mode order
$\mathbf{p}$	=	vector of pressure values for a given frequency f
$\mathbf{S}_{cc}$	=	cross-spectral matrix of mode or wavenumber coefficients
$\mathbf{S}_{pp}$	=	cross-spectral matrix of pressure at frequency f
$\mathbf{W}$	=	diagonal matrix of weights in the IBIA approach
η	=	regularization parameter
$\mathbf{\Phi}$	=	matrix that models the transfer function between pressure measured at the microphones and the duct modes
$\mathbf{\Psi}^{\ddagger}$	=	regularized inverse matrix
$\cdot^H$	=	conjugate transpose or Hermitian operator
$\mathbb{E}(\cdot)$	=	expected value
$\|\|\mathbf{x}_l\|\|_2^4$	=	the l_2 or Euclidean norm of the vector $\mathbf{x}$ to the 4th power

II. Introduction

The loudest aircraft engine ever developed was probably the Republic Aviation Corporation's XF-84H, an experimental F-84 Thunderjet fighter produced in 1955 for the US Air Force. Nicknamed "Thunderscreech," the sound pressure emanating from it was never officially recorded, but during initial testing at Edwards Air Force Base in California there were noise complaints from as far as 25 miles away and anyone caught in the propwash would vomit, faint, and/or

*PhD Student, Laboratoire de Mechanique des Fluids et d'Acoustique (LMFA)
†Engineer, LMFA
‡Professor, LMFA

collapse into seizures. Eventually the negative effects of the engine noise became so overwhelming that the base commander ordered that the testing be moved to a dry lake bed insulated by a large ridge [1].

Although we have come a long way from the highspeed turboprop days of the 1950s, noise reduction is still an important factor in aircraft design. Quieter turbofans may have replaced turboprops as the primary jet engine of choice [2], but they have their own unique noise-generation problems that require study to reduce. For example, instead of producing majority tonal-noise based profiles, turbofans tend to produce large amounts of broadband noise, reaching up to 90% of the profile at approach [3].

Since the sound field produced by a ducted engine can be expressed as a weighted sum of its modes, when it comes to noise reduction of aircraft it is important to know the acoustic modes propagating through the engines [4]. Although accurate analytical models of acoustic mode propagation exist for ducts with constant, unvarying cross-sections, similar models do not yet exist for more complex geometries that can feature varying diameters, unique rotor/stator configurations, liners, and etc. This causes it to not always be possible to know a priori the modes running through a turbofan duct under flight conditions. Additionally, Ganz *et al.* [5] wrote in 1998 that numerical simulations lack the ability to fully reproduce the range and detail of empirical data, and that a semi-empirical approach appears to be the most effective method for estimating blade noise from ducted fans.

The theory behind empirical modal reconstruction from far-field measurements has existed for decades. Tyler and Sofrin [6] began developing models for the cyclic part of engine acoustic radiation during the early 1960s. Initially this tonal noise was the focus of most acoustic radiation research, although as liners became more and more effective in attenuating this radiation eventually broadband noise reduction began to play a more important role in aircraft design. In 1974 Snow [7] found that attenuation of the broadband noise was dependent on knowing the sound field at the entrance to all acoustically treated engine sections, which almost invariably includes the inlet. As a result, in 1977 Lowrie and Morfey [8] developed a theory for determining the sound field at an engine inlet. In order to avoid disturbing the flow with in-duct measurements, they used a system that recreated the internal modes based on external pressure measurements. Tester *et al.* [9] then put this theory into practice in 1979 with a polar array of microphones arranged on a horizontal plane in front of an engine inlet to encouraging results.

Although the results were encouraging, the process of getting them was a difficult one. Lowrie and Morfey highlighted the problems associated with deviations in the microphone placement, especially in the radial direction. These problems were addressed in 2010 by Doebler *et al.* [10], who described multiple methods for the real-time determination of microphone coordinates. Their system was shown to be reasonably accurate, even when calibrating collapsible arrays in the field.

Other advances in microphone manipulation led to Enghardt et al [11] developing techniques for using in-duct arrays to measure sound power as part of mode detection experiments. They used wall-mounted and raked microphones and their techniques are projected to work even for Mach numbers up to 0.6, which means they are applicable for most model fan test benches.

Work on the inverse problem based on external measurements was undertaken by Lewy [12, 13] as early as 2004. He found that the inverse problem was ill-posed, citing there being no reason why a given directivity field should be uniquely defined as his rationale. Additionally, solutions will be underdetermined if there are more modes than microphones. To correct for this, Lewy suggested selecting modes a priori, then adjusting the mode amplitudes until the numerical results matched experimentally measured SPLs at similar angles and using a least squares fit to find the final solution. Another solution is to move the microphone array, which would allow one to measure the radiated pressure from additional locations.

External arrays and their use in the inverse problem were further improved in 2006 and 2007 by Castres and Joseph [14, 15], who worked primarily with radiated broadband noise. They tested several microphone layouts for the external array, and found that a uniform distribution of microphones in both the azimuthal and polar directions gave the most accurate coupling between the modal information and the sensor positions. The authors proposed that this geodesic dome of microphones could be mounted behind a turbulence control screen (TCS) or even directly on it. Furthermore, they proposed combining pressure results from microphone arrays both inside and outside of the conduit in order to produce a working transfer function between the internal modes and the external measurements.

There are multiple methods of mode reconstruction from microphone data. These include beamforming, Bayesian approaches, Fourier decomposition, deconvolution approaches, pseudo inverse methods, neural networks, CLEAN, etc [16, 17]. Beamforming is the standard method used for reconstruction of source noise from microphone data [18]. Types of beamforming have been around since as early as World War I, when French forces used rotatable listening devices to detect approaching aircraft [19], and German troops donned acoustic-locating hats [20]. The first suggestion of beamforming using an array of microphones placed in an antenna appeared in a 1974 paper by John Billingsley, who put his suggestion into practice with Kinns in 1976 to study the noise emission of a Rolls-Royce/SNECMA Olympus engine, which was used at the time by aircraft produced by Concorde.

Conventional beamforming methods have been well-studied for broadband noise mode reconstruction [17]. It was developed based on least-squares optimization, which means that the resolution can be subject to contamination between mutual modes under certain conditions. This leads to a small dynamic range for this method, although there are algorithms that can mitigate this, such as CLEAN-SC.

Another method is the one described by Pereira and Jacob [16], which is based on an iterative Bayesian inverse approach (IBIA). Like beamforming, Bayesian approaches have historically been used in the field of acoustics primarily for source localization. Unlike beamforming, it does not require the assumption of incoherence between modes, and it was only very recently that this method has begun to be used for mode reconstruction, with Roncen et al [21] using this method in 2019 to successfully determine the mode amplitudes and flow profiles of synthetic noise signals. Compared to least-squares beamforming (LSA), IBIA has been shown to offer such benefits as reduction of artifacts in the array sidelobes, improvement of the dynamic range, more control of the sparsity, and can be applied directly with the cross-spectral measurement matrix. Addtionally, while many methods are either good for broadband or tonal noise reconstruction, IBIA works reasonably well with both.

In order to reconstruct modal behavior inside a duct from external pressure measurements, it is necessary to derive a working transfer function. The method investigated in this study is the use of an external system of microphones attached to a geodesic array surrounding the front half of an engine inlet. Results are confirmed by use of an internal microphone array, while the transfer functions are derived with the help of numerical models. The experimental rig is presented in Section 2, the procedure for reconstructing the modes is included in Section 3, the numerical simulations are included in Section 4, and finally the preliminary results are included in Section 5.

III. Test Bench

For its test rig this study uses the LP3 engine, which is an axial, low-speed, ducted fan run by the Laboratoire de Mécanique des Fluides et d'Acoustique at the Ecole Centrale de Lyon. It was designed and manufactured by Safran Ventilation Systems, and a picture of the engine in the facility can be seen in Fig. 1 [22]. The LP3 test bench features a maximum flow speed of 40 m/s, a Bellmouth inlet of unique design, a turbulence control screen, multiple temperature and pressure sensors, 13 acoustic sources, and both external and internal microphone arrays, while the room is equipped with movable acoustic shielding on the walls, the floor, and separating the duct inlet and external array from air released out of the outlet. A list of the frequencies for the first three BPFs in the LP3 for the nominal rotational speed of 9800 rpm is given in Table 1.

Table 1 List of BPFs in the LP3 at 9800 rpm

BPF Number	**1**	**2**	**3**
Frequency (Hz)	2796	5592	8388

A. Microphone Arrays

Two of the LP3 microphone arrays have been used for this project. One is an external design, which contains 89 microphones mounted on a geodesic dome that surrounds the front half of the duct inlet. A picture of this formation is given in Fig. 2.

This dome was developed specifically for use in mode reconstruction via external measurements. Several design variations were considered before settling on the given configuration. Much like Castres and Joseph[15], it was found that a geodesic dome was the best solution, although different lengths were preferred, and the microphones were placed at a distance of 0.7 m from the duct opening. Built with carbon fiber rods (black) for rigidity, the microphone holders (white) were created using a 3D printer and the entire structure is directly connected to the TCS at the base, which helps for positioning and stability. The microphones were placed and their positions were verified using a 3D printed distance tool and a laser, and calibrations were undertaken using a source with a steady frequency of $f = 1000$ Hz.

The second array used for this modal reconstruction effort is internal. It contains 53 microphones and is located very close to the duct edge, where it is a sufficient distance from the fan portion of the engine so that non-propagating

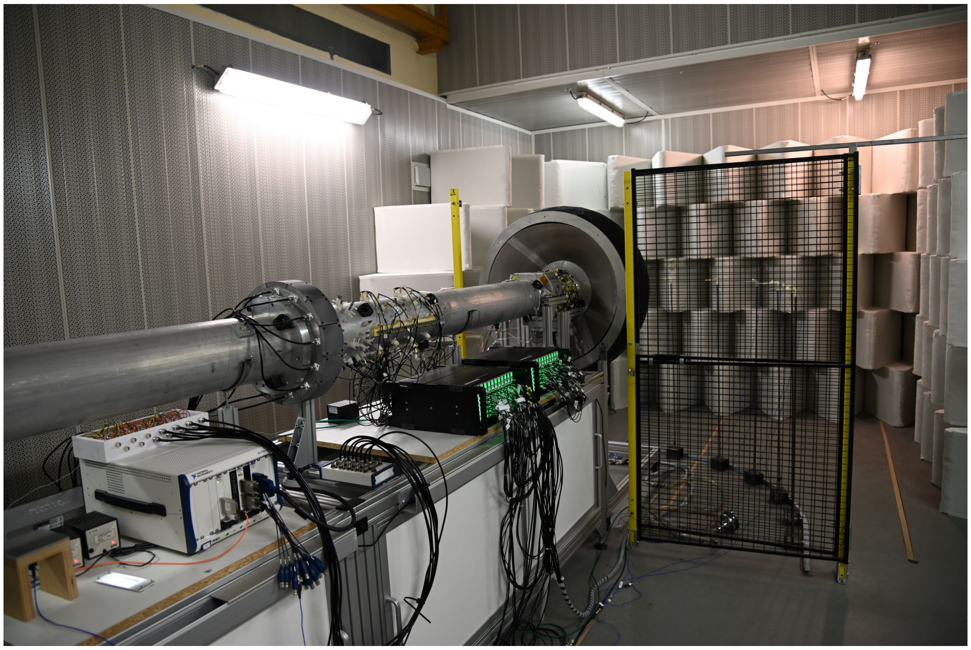

Fig. 1 View of the LP3 test rig

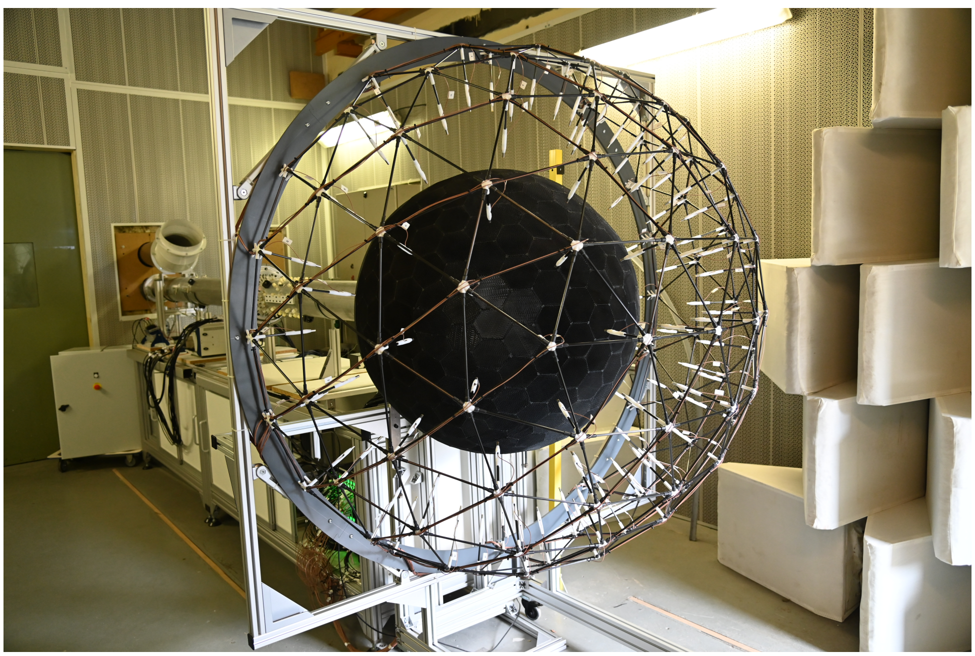

Fig. 2 External microphone array for the LP3 test bench

modes will not be detected. Featuring recessed, pinhole microphones that are embedded in the conduit side, this array can be seen in Figure 3. These pinhole microphones were chosen over raked or wall-flush microphones in order to avoid generating turbulence in the inlet and boundary layer effects.

Positioning of the internal array is easy: the microphones are mounted directly onto the duct, with pinholes drilled into the conduit, and do not move once installed. The backs of the microphones, which stick out of the metal walls of the duct, are firmly screwed down and are protected from the flow by the Bellmouth inlet.

Due to processing constraints, not all of the microphones could be used simultaneously, so some tests were run with

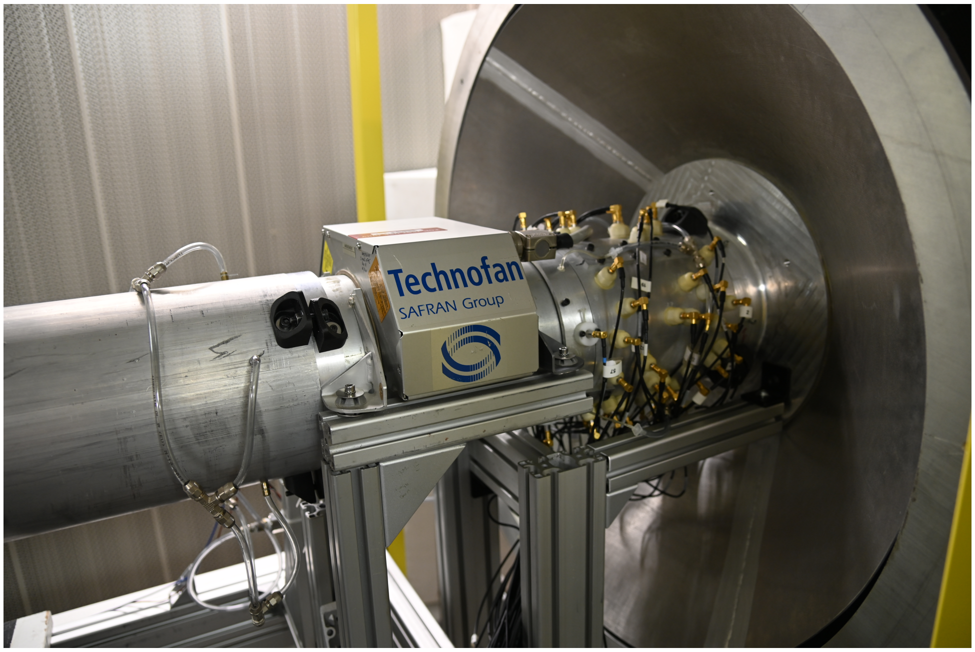

Fig. 3 View of the internal microphone array

the full external array and others with the full internal array. A comparison of the data procured by these arrays to numerical simulations is given in Section 6.

IV. Modal Analysis Approach

The quantity measured by the microphones is the acoustic pressure field, which can be expressed as a weighted sum of duct modes [16]. This leads to the generation of a linear system of equations that can be written in matrix-vector notation such as shown in Eq 1 .

$$\mathbf{p} = \boldsymbol{\Phi c} \tag{1}$$

In this equation $\mathbf{p}$ is the pressure in vector form, Φ is the transfer function - a matrix that is determined analytically for the in-duct array but which must be determined numerically for the external array, and $\mathbf{c}$ is the vector of mode amplitudes. The pressure is found experimentally and the mode coefficient vectors are the unknowns. Equation 1 can be written in terms of the cross-spectral matrix of measurements ($\mathbf{S}_{pp} \triangleq \mathbb{E}\mathbf{pp}^H$), which brings about the following equation:

$$\mathbf{S}_{pp} = \boldsymbol{\Phi} \mathbf{S}_{cc} \boldsymbol{\Phi}^H \tag{2}$$

The interesting quantities in this formula are the squared moduli of the modes amplitudes, which are the diagonal terms of $\mathbf{S}_{cc}$. Off-diagonal terms are the cross-spectra between modal coefficients and become interesting when coherence between modes is expected, such as for tonal noise. Multiple methods can be used for determining the value of $\mathbf{S}_{cc}$. Beamforming is the classic approach that has often been used, although recently new techniques have been being applied instead. One of the more recent systems is an iterative Baysian inverse approach (IBIA) developed by Pereira and Jacob [16].

A. Conventional Beamforming

Beamforming was one of the first tools to be used for modal analysis. It typically uses a least squares approach (LSA) and assumes that the sources are incoherent, which leads to the solution coefficients being written as

$$\hat{c}_l = \frac{\phi_l^H \mathbf{S_{pp}} \phi_l}{||\phi_l||_2^4} \tag{3}$$

where ϕ_l is the lth column of matrix $\mathbf{\Phi}$ and the notation $||\mathbf{x}_l||_2^4$ denotes the l_2 or Euclidean norm of the vector $\mathbf{x}$ to the 4th power. Although this method gives values for the $\hat{S}_{cc}$ matrix coefficients, it does not give a full estimate of all of the values because it starts from the assumption of incoherence between the modes. Additionally, beamforming is known for having limited resolution and poor quantification results. This is why a different approach was considered.

B. Iterative Bayesian Inverse Approach

IBIA, on the other hand, does not start from an assumption of incoherence. By allowing for coherence between modes, it is better able to reproduce what is observed experimentally. This provides it a broader resolution, but at a higher computational cost. Other benefits of this method include that it supports user-defined sparsity control and it permits users to automatically adjust the regularization parameter (η) - an explanation of how to intrinsically find η can be found in the paper by Pereira et al [23]. This approach begins from the typical Bayesian assumption that all variables in a problem are stochastic processes, and proceeds from there. The full derivation of IBIA can be found in [16].

The IBIA solution to this problem can be written as:

$$\hat{\boldsymbol{c}} = \ulcorner \boldsymbol{W} \lrcorner^2 \mathbf{\Phi}^{\boldsymbol{H}} (\mathbf{\Phi} \ulcorner \boldsymbol{W} \lrcorner^2 \mathbf{\Phi}^{\boldsymbol{H}} + \boldsymbol{\eta}^2 \mathbf{I})^{-1} \mathbf{p} \tag{4}$$

where $\mathbf{W}$ is a diagonal matrix with generic elements $w_i = |\hat{c}_{i,k-1}|^{1-\frac{p}{2}}$, $\hat{c}_i$ is the i-th element of vector $\mathbf{c}$, η is the regularization parameter, and $\mathbf{I}$ is the identity matrix. The solution to Eq. 4 may by written in terms of $\mathbf{S}_{pp}$ as:

$$\hat{\boldsymbol{S}}_{\boldsymbol{cc}} = \mathbf{\Psi}^{\ddagger} \mathbf{S}_{\boldsymbol{pp}} (\mathbf{\Psi}^{\ddagger})^{\boldsymbol{H}} \tag{5}$$

where $\mathbf{\Psi}^{\ddagger}$ is a regularized inverse matrix defined as

$$\mathbf{\Psi}^{\ddagger} = \ulcorner \boldsymbol{W} \lrcorner^2 \mathbf{\Phi}^{\boldsymbol{H}} (\mathbf{\Phi} \ulcorner \boldsymbol{W} \lrcorner^2 \mathbf{\Phi}^{\boldsymbol{H}} + \boldsymbol{\eta}^2 \mathbf{I})^{-1} \tag{6}$$

V. Numerical Calculation of the Transfer Function

Numerical simulations are necessary to find the transfer function and subsequently the mode amplitudes. Analytical solutions only exist for very basic duct configurations, and it was shown in the paper by Ford *et al* [24] that duct lip geometry has a large impact on external pressure measurements. As such, numerical simulations are imperative when considering any conduit configuration that deviates from the basic standard. This project intends to conduct mode reconstruction using a complex duct inlet of unique design, so to do this the LP3 duct geometry and external microphones were modeled using the software Actran TM: a finite element program that specializes in acoustic phenomena. This software can be controlled using a visual interface or by way of a python-based interface panel and has been designed to predict acoustic physical behavior for situations which are difficult to determine analytically. To run its simulations, Actran extrapolates solutions primarily using Möhring's Equation [25].

A. Mesh Geometry

Figure 4a shows the mesh of the axisymmetric configuration, which consists of the air surrounding and inside the duct entrance. The shape of the Bellmouth inlet is visible as the edge of the mesh, and the length of the acoustic fluid in front of the duct lip was chosen to accommodate multiple wavelengths of the acoustic signal, even at high frequency and high velocity. Additionally, the density of the finite elements follows a gradient that is highly packed near the curve where the Bellmouth meets the duct and becomes less crowded the further one moves from the inlet.

The microphones in the external array are shown in the model with red field points. A second image from the front of the conduit is included in Fig. 5b to show a different perspective on the array. In order to avoid reflections at the far border of the mesh, a pressure propagation extrapolation method must be employed. For this computation, infinite elements were chosen. An explanation of the choice behind this element type can be found in the paper by Ford et al[24].

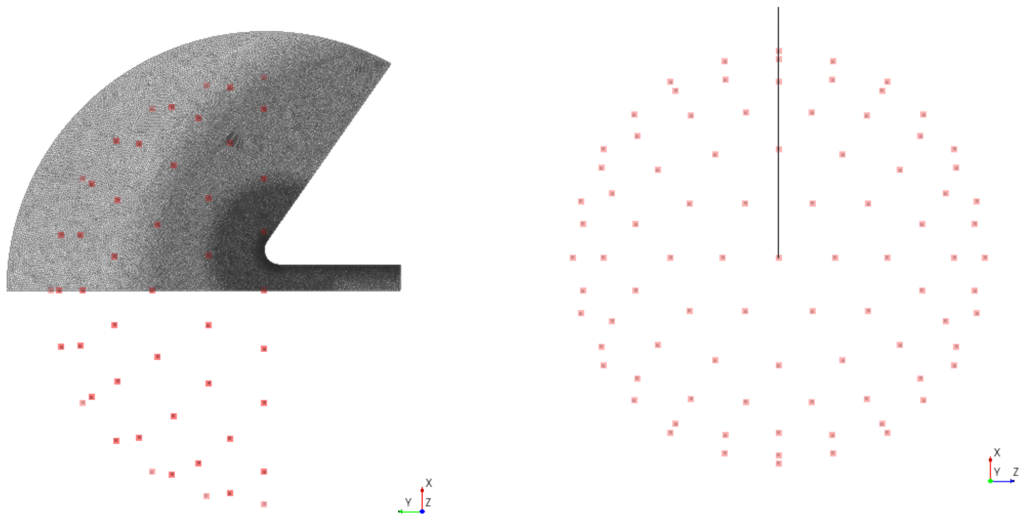

(a) **(b)**

Fig. 4 The full 2D axisymmetric mesh from the side (a) and the front (b)

B. Simulation Variables

Simulations were carried out with frequencies around the first three BPFs, the values for which are given in Table 1. All of these windows included 11 frequencies spaced 8 Hz apart, covering a total of 80 Hz. Flow was included using Actran's potential flow solver: the Compressible Flow Analysis (CFA). For these simulations, velocity, velocity potential, and the temperature are specified. All of these values were chosen to match experiment: the top speed of the air moving through the duct was calculated to be 37.97 m/s, the velocity in the farfield was 0 m/s, the velocity potential in the farfield was specified with a value of 0 m^2/s, and the temperature in the farfield was measured as 20.2 °C. The calculated velocity profile at nominal rotational speed is shown in Fig. 5. Simulations for both positive and negative spinning modes were performed, and all mode amplitudes were set to one to give a direct correspondence to the transfer matrix. Finally, a complete list of important parameters that were used for these simulations is given in Table 2.

Table 2 List of applied numerical parameters

Variable	Configuration
Interpolation Order	Quadratic
Extrapolation Method	Infinite elements
Frequency Range	80 Hz windows around the first 3 BPFs in increments of 8 Hz
Speed of Sound	342.75 m/s
Air Density	1.16 kg/m^3
Mode Splitting	Positively and negatively rotating modes

It is possible to visualize the acoustic pressure moving through the fluid in the duct. The pattern of pressure waves exiting the LP3 geometry inlet for the planewave mode is presented in Figure 6a and for the (0,1) mode in Figure 6b. These graphs demonstrate that different modes have different propagation patterns, and that it is possible to distinguish modes based on their movement through the conduit. They also show that there is a lot of forward radiation for the planewave mode, but that for other modes the radiation is lower directly in front of the inlet and higher towards the side.

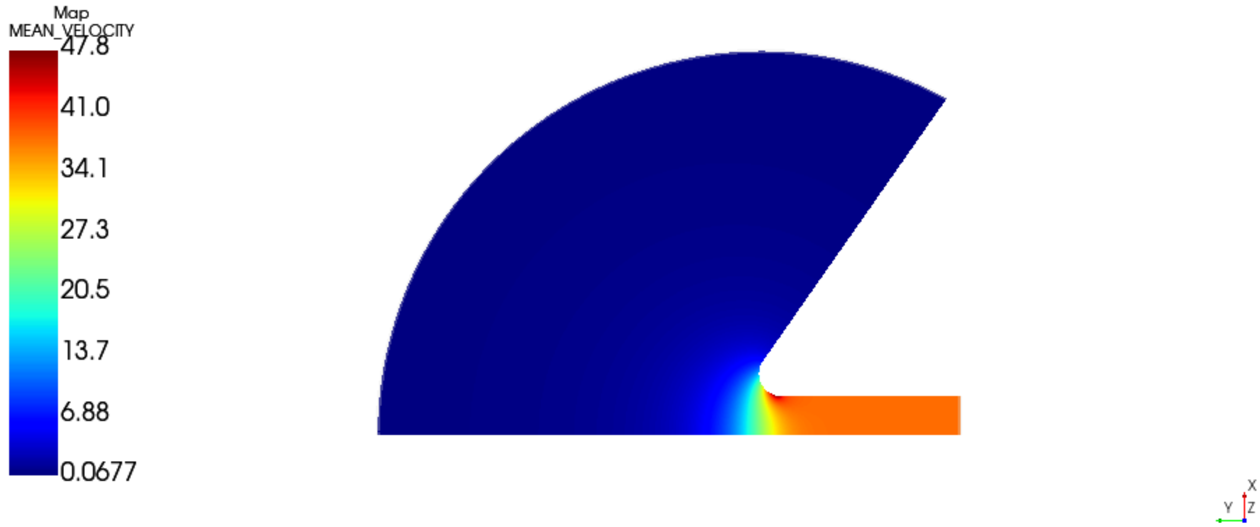

Fig. 5 Velocity profile for all CFA simulations

VI. Experimental Results

Mode reconstruction was performed for the external array using pressure measurements and the matrix generated by the numerical simulations. These reconstructed external modes then were compared to the modes found using the internal array, which were found using a matrix derived from the analytical solution of a rigid-walled circular duct. Results for the first BPF for both the external and internal arrays are included in Figure 7, and the graphs show the total pressure for each azimuthal mode. These azimuthal mode pressures are calculated by adding the pressure for all of the radial modes with the same azimuthal order.

Flow speed through the duct was calculated using the mass flow rate of the incoming air, and both of these values are also listed in the following table. When flow is included in the simulations, one extra mode is found compared to simulations without flow. This mode is the (m=2,n=3) mode, where m is the azimuthal mode order, and n is the radial mode order.

As the first BPF graphs demonstrate, both the internal and external arrays find the same dominant acoustic modes propagating through the LP3 conduit. The $m = -3$ mode has the highest measured pressure, followed by the $m = +3$ mode, although the external array reconstruction found that the $m = +3$ mode was proportionally weaker than the internal version.

The modes for the second BPF are given in Figure 8. For this frequency the two dominant values are for the m=+5,+7 modes. However, in this case, although both methods find the same two dominant modes, they find that the most dominant and second most dominant are switched, with the internal array finding that the m=+5 mode is the most dominant, and the external array finding that the m=+7 is the most dominant.

VII. Conclusion and Perspectives

In order to reconstruct acoustic modes propagating out of a conduit with unique geometry from external measurements, a transfer function can be generated numerically to solve the inverse problem. This paper detailed how to produce the transfer function, how to use the function in an iterative Bayesian inverse approach to reconstruct modes using external measurements, and finally compared the IBIA-produced reconstructed modes with results obtained from measurements taken directly inside the duct of the LP3 engine for the first two BPFs to determine the viability of this approach.

For the first BPF, the external array/IBIA approach produces a mode reconstruction pattern that almost exactly matches the pattern found by the internal array, with the m=-3 modes highly dominant, the m=+3 modes next in line, and the other modes barely contributing to the acoustic pressure. For the second BPF, the mode reconstruction patterns vary slightly, but both arrays find the same two modes as the dominant pair, albeit switched in intensity, with the

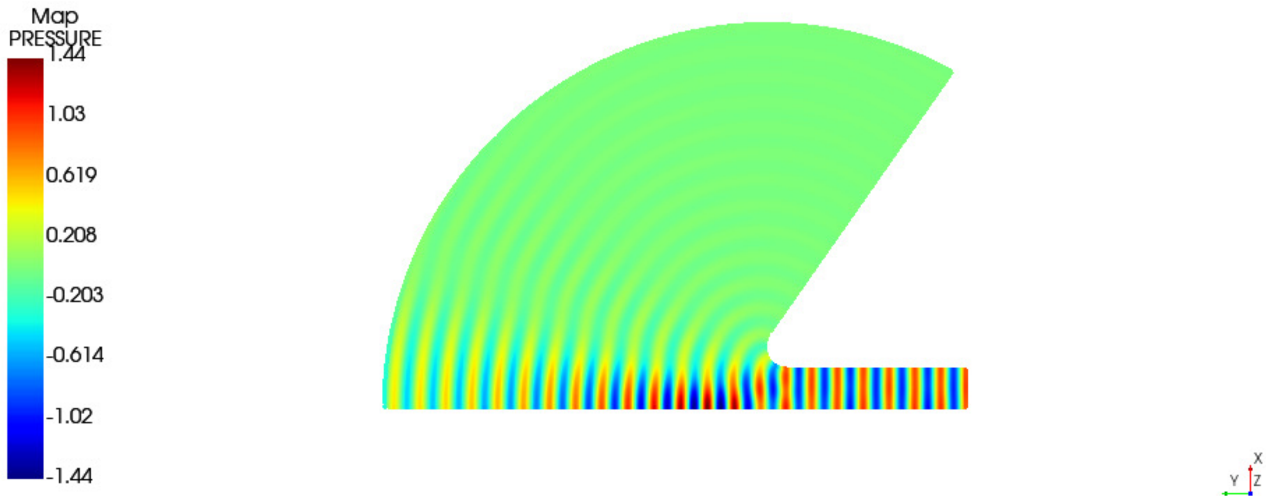

(a)

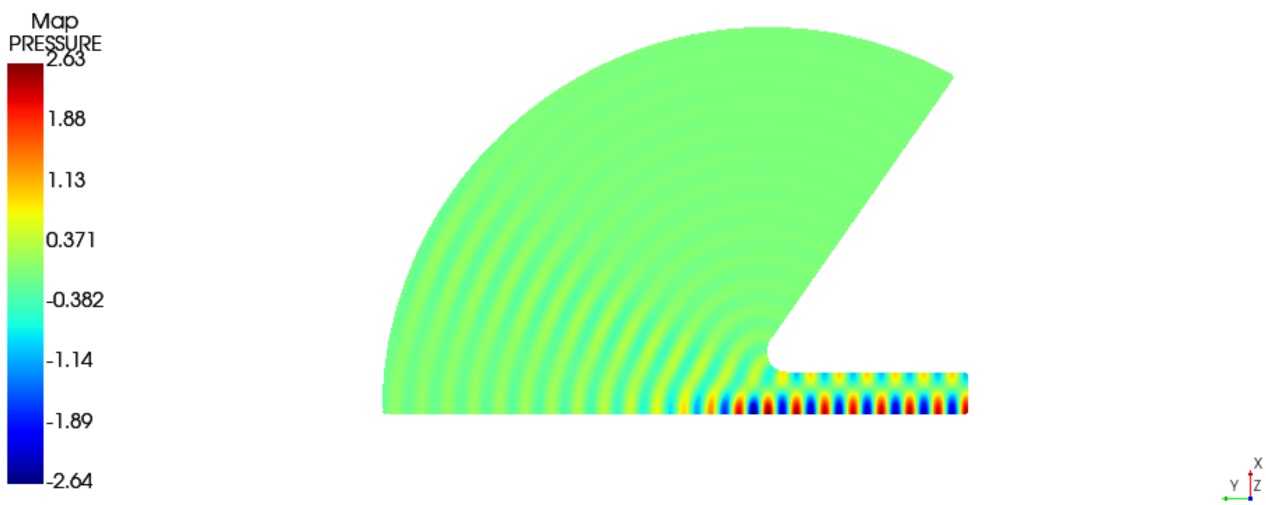

(b)

Fig. 6 Acoustic pressure profiles in the fluid for the (a) planewave and (b) (0,1) modes

external/IBIA approach calculating the m=+7 modes to be dominant followed closely by the m=+5, and the internal array measuring the m=+5 modes to be dominant followed closely by the m=+7. Some of the possible reasons for the small discrepancies between the external/IBIA results and the internal results could be modes being close to cut-off, so that they are found by the internal array but not the external array, modes being reflected back into the duct or split into other modes when reaching the inlet edge, and internal microphones measuring evanescent modes.

Despite some small differences in the reconstructions, the patterns from both the external array/IBIA approach and

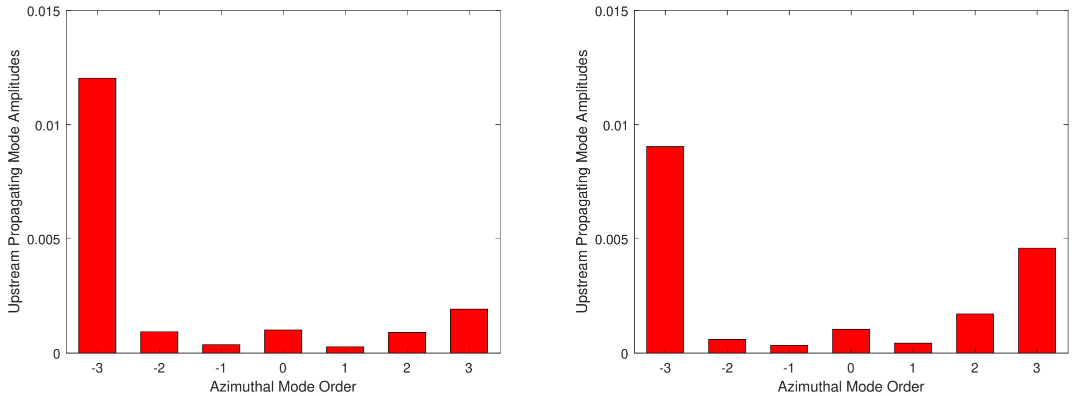

(a) **(b)**

Fig. 7 Mode reconstruction for the first BPF from the external array (a) and the internal array (b)

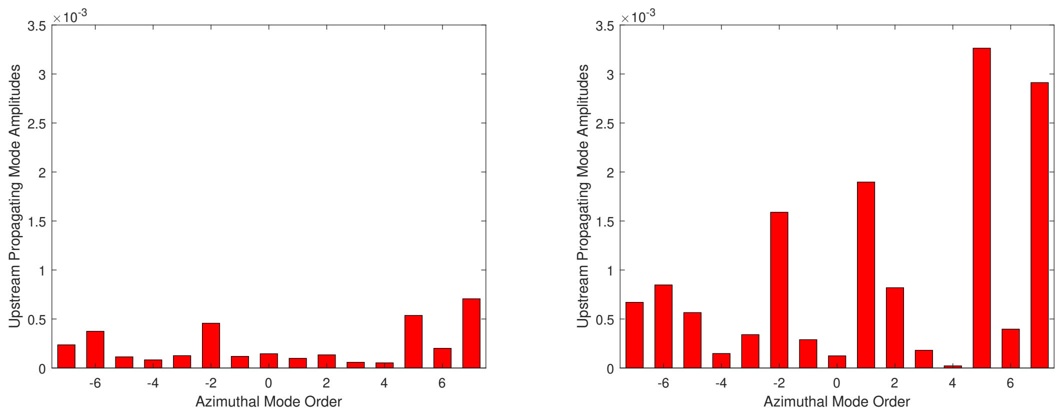

(a) **(b)**

Fig. 8 Mode reconstruction for the second BPF from the external array (a) and the internal array (b)

the internal array are very similar in form. Further investigation will be conducted in order to better understand the differences. Such phenomena as evanescent modes and their effect on in-duct array post-processing as well as acoustic reflections from surfaces in the testing facility and how these reflections affect external measurements will be studied. Additionally, predictions of pressure measurements and modal content based on this procedure will be considered.

Acknowledgments

This work was performed within the framework of the industrial chair ARENA (ANR-18-CHIN-0004-01) co-financed by Safran Aircraft Engines and the French National Research Agency (ANR). Funding was also provided by the Labex CeLyA (ANR-10-LABX-0060) of the Université de Lyon, within the program "Investissements d'Avenir" (ANR-16-IDEX-0005) operated by the ANR.

References

[1] "Loudest Aircraft," , 2022. URL `https://www.guinnessworldrecords.com/world-records/633410-loudest-aircraft`.

[2] Gerhold, C. H., Cabell, R. H., and Brown, D. E., "Generation of Higher Order Modes in a Rectangular Duct," *Williamsburg, Virginia Active 04*, 2004.

[3] "TurboNoiseBB," , 2022. URL `https://dlr.de/at/desktopdefault.aspx/tabid-12815/22389_read-53176/`.

[4] Castres, F., Joseph, P., and Astley, J., "Mode Detection in Turbofan Inlets from Acoustic Pressure Measurements in the Radiated Field," *10th AIAA/CEAS Aeroacoustics Conference*, American Institute of Aeronautics and Astronautics, 2004. https://doi.org/10.2514/6.2004-2953.

[5] Ganz, U., Glegg, S., and Joppa, P., "Measurement and prediction of broadband fan noise," *4th AIAA/CEAS Aeroacoustics Conference*, American Institute of Aeronautics and Astronautics, 1998. https://doi.org/10.2514/6.1998-2316.

[6] Tyler, J. M., and Sofrin, T. G., "Axial Flow Compressor Noise Studies," *SAE Technical Paper Series*, SAE International, 1962. https://doi.org/10.4271/620532.

[7] Snow, D., "Influence of source characteristics on sound attenuation in a lined circular duct," *Journal of Sound and Vibration*, Vol. 37, No. 4, 1974, pp. 459–465. https://doi.org/10.1016/s0022-460x(74)80026-x.

[8] LOWRIE, B., and MORFEY, C., "Far-field methods of duct mode detection for broad-band noise sources," *4th Aeroacoustics Conference*, American Institute of Aeronautics and Astronautics, 1977. https://doi.org/10.2514/6.1977-1331.

[9] TESTER, B., CARGILL, A., and BARRY, B., "Fan noise duct-mode detection in the far-field - Simulation, measurement and analysis," *5th Aeroacoustics Conference*, American Institute of Aeronautics and Astronautics, 1979. https://doi.org/10.2514/6.1979-580.

[10] Doebler, D., Heilmann, G., and Ohm, M., "Automatic Detection of Microphone Coordinates," *Berlin Beamforming Conference 2010*, February 2010.

[11] Enghardt, L., Neuhaus, L., and Lowis, C., "Broadband Sound Power Determination in Flow Ducts," *10th AIAA/CEAS Aeroacoustics Conference*, American Institute of Aeronautics and Astronautics, 2004. https://doi.org/10.2514/6.2004-2940.

[12] Lewy, S., "Inverse method predicting spinning modes radiated by a ducted fan from free-field measurements," *The Journal of the Acoustical Society of America*, Vol. 117, No. 2, 2005, pp. 744–750. https://doi.org/10.1121/1.1850208.

[13] Lewy, S., "Numerical inverse method predicting acoustic spinning modes radiated by a ducted fan from free-field test data," *The Journal of the Acoustical Society of America*, Vol. 124, No. 1, 2008, pp. 247–256. https://doi.org/10.1121/1.2931952.

[14] Castres, F. O., and Joseph, P. F., "Mode Detection in Turbofan Inlets from Near Field Sensor Arrays," *The Journal of the Acoustical Society of America*, 2006. https://doi.org/10.1121/1.2427124.

[15] Castres, F. O., and Joseph, P. F., "Experimental Investigation of an Inversion Technique for the Determination of Broadband Duct Mode Amplitudes by the Use of Near-Field Sensor Arrays," *The Journal of the Acoustical Society of America*, 2007. https://doi.org/10.1121/1.2747166.

[16] Pereira, A., and Jacob, M. C., "Modal analysis of in-duct fan broadband noise via an iterative Bayesian inverse approach," *Journal of Sound and Vibration*, Vol. 520, 2022, p. 116633. https://doi.org/10.1016/j.jsv.2021.116633.

[17] Suzuki, T., and Day, B. J., "Comparative study on mode-identification algorithms using a phased-array system in a rectangular duct," *Journal of Sound and Vibration*, Vol. 347, 2015, pp. 27–45. https://doi.org/10.1016/j.jsv.2013.06.027.

[18] Michel, U., "History of Acoustic Beamforming," *Berlin Beamforming Conference 2006*, 2006.

[19] Heilmann, G., Doebler, D., and Boeck, M., "Exploring the Limitations and Expectations of Sound Source Localization and Visualization Techniques," *Inter.Noise Melbourne Australia 2014*, 2014.

[20] "Aircraft detection before radar, 1917-1940," , 2021. URL https://rarehistoricalphotos.com/aircraft-detection-radar-1917-1940/.

[21] Roncen, R., Méry, F., and Piot, E., "Bayesian inference for modal identification in ducts with a shear flow," *The Journal of the Acoustical Society of America*, Vol. 146, No. 4, 2019, pp. 2645–2654. https://doi.org/10.1121/1.5130195.

[22] Pestana, M., Pereira, A., Salze, E., Thisse, J., Sanjose, M., Jondeau, E., Souchotte, P., Roger, M., Moreau, S., Regnard, J., and Gruber, M., "Aeroacoustics of an axial ducted low Mach-number stage: numerical and experimental investigation," *23rd AIAA/CEAS Aeroacoustics Conference*, American Institute of Aeronautics and Astronautics, 2017. https://doi.org/10.2514/6.2017-3215.

[23] Pereira, A., Antoni, J., and Leclere, Q., "Empirical Bayesian Regularization of the Inverse Acoustic Problem," *J Acous Soc Am*, 2015.

[24] Ford, C., Pereira, A., and Bailly, C., "Radiation of Higher Order Modes from Circular Ducts with Flow," *unpublished*, 2022.

[25] *Actran 19.1 User's Guide Volume 2 Extended DAT Input File Syntax*, 2019.